Received: 4 December 2023 | Accepted: 29 February 2024

DOI: 10.1002/pgr2.19

ORIGINAL RESEARCH

Proteoglycan Research WILEY

A novel biomimetic probe for galectin-3 recognition: Chemical synthesis and structural characterization of a β-galactose branched sodium hyaluronate

Sofia Nizzolo[1,2] | Emiliano Esposito[1] | Ming-Hong Ni[1] | Laura Bertocchi[3] | Giulio Bianchini[4] | Nadia Freato[3] | Serena Zanzoni[5] | Marco Guerrini[1] | Sabrina Bertini[1]

[1]Istituto di Ricerche Chimiche e Biochimiche G. Ronzoni, Milan, Italy

[2]University of Milano-Bicocca, Milan, Italy

[3]Glycocore Pharma Srl, Como, Italy

[4]JoinTherapeutics Srl, Padova, Italy

[5]Centro Piattaforme Tecnologiche, University of Verona, Verona, Italy

Correspondence
Sabrina Bertini, Istituto di Ricerche Chimiche e Biochimiche G. Ronzoni, Milan 20133, Italy.
Email: bertini@ronzoni.it

Funding information
Non-Profit Research Foundation "Istituto di Ricerche Chimiche e Biochimiche G. Ronzoni."

Abstract

Sodium hyaluronate (HA), a derivative of hyaluronan, is a natural and biocompatible polysaccharide that interacts with cluster of differentiation-44 receptor to promote fine-tuning of inflammation, fibrosis, and tissue remodeling. HA has a smaller molecular weight than hyaluronan and is overall more stable being less prone to oxidation. In this study, we report a novel lactose-functionalized sodium hyaluronate, named HYLACH®. Functionalization with multiple β-galactose residues facilitates its interaction with galectin-3, a β-galactose binding lectin implicated in various pathological processes including inflammation, host defense, and fibrosis, especially critical in idiopathic pulmonary fibrosis (IPF). Our strategy was to modify HA, to varying extents, at carboxyl sites with 1-amino-1-deoxy-lactitol, in the presence of 4-(4,6-dimethoxy-1,3,5-triazin-2-yl)-4-methyl morpholinium chloride in aqueous media. We characterized the chemical structure, molecular weight, and degree of substitution of HYLACH® using NMR spectroscopy and size exclusion chromatography. We further determined several key parameters including its stability toward enzymatic degradation and the binding affinity and conformational changes of galectin-3 interaction with HYLACH®. Collectively, the generation of a novel functionalized HA with an ability to bind and suppress galectin-3 function, in combination with safety and biocompatibility, offers the opportunity to test this compound in therapeutic trials of devastating fibrotic diseases such as IPF.

KEYWORDS

galectin-3, hyaluronidase, HYLACH®, isothermal titration calorimetry, molecular weight distribution, NMR, sodium hyaluronate

Abbreviations: BAL, broncho-alveolar lavage; CD, circular dichroism; CD-44, cluster of differentiation-44; CRD, carbohydrate recognition domain; DMTMM, 4-(4,6-dimethoxy-1,3,5-triazin-2-yl)-4-methyl morpholinium chloride; DS, degree of substitution; ECM, extracellular matrix; GAG, glycosaminoglycan; Gal-3, galectin-3; GlcA, glucuronic acid; GlcNAc, *N*-acetyl-β-D-glucosamine; HA, sodium hyaluronate; HP-SEC-TDA, high-performance size exclusion chromatography with triple detector array; HYAL, hyaluronidase; IPF, idiopathic pulmonary fibrosis; ITC, isothermal titration calorimetry; LAC-NH_2, 1-amino-1-deoxy-lactitol; OHA, HA oligomers; OHY, HYLACH oligomers.

INTRODUCTION

Biopolymers are abundant in nature and have gained popularity in the pharmaceutical industry due to the advantages they offer. They are nontoxic and biocompatible, facilitating their use as versatile scaffolds or carriers in drug delivery applications. Sodium hyaluronate (HA) is a linear, nonsulfated polysaccharide which belongs to the glycosaminoglycan (GAG) family.[1,2] HA is naturally occurring in vertebrates and invertebrates as a component of mucus or joint fluids, and in the extracellular matrix (ECM).[3,4] HA offers biocompatibility, biodegradability, and low immunogenicity, and plays a role in tissue hydration and elasticity owing to its high water retaining capacity, and to its viscoelasticity properties.[5] In addition, HA also interacts with the cell receptor cluster of differentiation-44, triggering biochemical processes that include cellular growth, proliferation, migration and adhesion, wound healing, and tumor metastasis.[1,6] In contrast to other GAGs, HA is structurally uniform as it comprises repeating disaccharide units of β-D-glucuronic acid (GlcA or G) and *N*-acetyl-β-D-glucosamine (GlcNAc or A) linked by (1,4) and (1,3) glycosidic bonds. Advances in biotechnology have made HA readily available in large quantities. Besides its intrinsic properties, HA can be functionalized and chemically modified to provide an even wider range of physical properties and chemical features. Some of the challenges of HA derivatization include overcoming its limited solubility in organic solvents and its sensitivity to harsh reaction conditions such as acidic or alkaline environments, or oxidative and thermal stress. Nevertheless, HA has been widely used in several pharmaceutical applications.[1] HA derivatization involves two principal functional sites: the carboxylic acid group and the hydroxyl group. A broad range of HA-based materials have been synthesized by various chemical methods in the form of conjugated or cross-linked HA for the enhancement, modulation, and control of its therapeutic action.[7]

Here, we describe the synthesis of HYLACH®,[8] a HA-based molecule conceived through a safe-by-design approach for the treatment of idiopathic pulmonary fibrosis (IPF), a rare disease characterized by rapid fibrosis progression leading to respiratory failure and death.[9,10] HYLACH® is a HA derivative designed to bind specifically galectin-3 (Gal-3), a key protein in fibrosis documented to be implicated in IPF.[11–13] Gal-3, encoded by the *LGALS3* gene, is a ~30 kDa protein member of the glycan-binding family of lectins. It contains a carbohydrate recognition domain (CRD) as well as an N-terminal oligomerization domain. Through the N-terminal domain, Gal-3 can oligomerize to form pentamers. Gal-3 binds β-D-galactose through its CRD, enabling it to bind β-galactose-terminated glycans or glycoproteins. Thanks to its ability to pentamerize, Gal-3 can cross-link complexes of the ECM to organize a dynamic lattice. [14] The roles of Gal-3 are broad, and it has been implicated in a plethora of biological processes. Recent literature has demonstrated that Gal-3 expression relates to myofibroblast proliferation, fibrogenesis, tissue repair, inflammation, and tissue remodeling. In a mouse model of bleomycin-induced fibrosis, Gal-3 was found to be overexpressed.[15] Furthermore, in a Gal-3 knock-out mouse model, a protective ability toward bleomycin-induced fibrosis was observed in comparison to wild-type mice.[16] Gal-3 has also been found to be overexpressed in the sera of IPF patients, as well as in broncho-alveolar lavage fluid, and in patients undergoing acute exacerbations.[16]

Given this growing evidence of the importance of Gal-3 in fibrosis and the intrinsic potential as a biomarker in fibrotic diseases including IPF, Gal-3 represents an appealing new candidate for IPF therapy. Two approved oral drugs, Pirfenidone and Nintedanib, are currently employed for the therapy of IPF, however, the adverse effects associated with the treatment often lead to the therapy being discontinued.[17]

HYLACH®, constructed on a HA backbone, offers improved biocompatibility compared to the currently available therapeutic options, combined with the ability to sequester Gal-3, thereby modulating fibrosis in lung disease. Functionalization of HA involves the derivatization with lactose (D-gal β(1-4)-D-Glc) moieties consisting of 1-amino-1-deoxy-lactitol (LAC-NH_2), covalently bound to the carboxylate groups of HA via an amide bond. The functionalization of HA with LAC-NH_2 in this manner ensures that the integrity of the β-D-configuration of the galactose ring is retained, thereby maintaining the possibility of interaction with Gal-3. HYLACH® has already been reported to attenuate macrophage-induced inflammation and inhibit Gal-3 expression among other ECM proteins, while also exhibiting antioxidative effects.[8] In addition, the superiority of HYLACH in comparison to HA in reducing both gene and protein expression of fundamental profibrotic molecules has been demonstrated.[18]

Two HA with different molecular weights (90 and 400 kDa) were employed. The chemical structure, molecular size, and stability toward enzymatic degradation of the synthetize products were characterized using NMR spectroscopy and size exclusion chromatography (SEC) with triple detector array (HP-SEC-TDA) techniques. To determine the degree of substitution (DS) of these high molecular weight polysaccharide derivatives, a strategy based on the use of two-dimensional (2D) NMR spectroscopy was developed. To confirm the binding and the putative inhibition of Gal-3 with HYLACH® oligomers, ITC, and circular dichroism (CD) were employed and the binding affinities with three known Gal-3 ligands (LAC-NH_2, galactose, and lactose) were compared.

MATERIALS AND METHODS

Materials

HA samples, nominal molecular weight average of 90 and 400 kDa were provided by HTL Biotechnology Javene. 4-(4,6-dimethoxy-1,3,5-triazin-2-yl)-4-methyl morpholinium chloride (DMTMM), α-D-lactose, ammonium hydroxide solution 28%–30%, sodium cyanoborohydride, ammonium acetate (NH_4OAc), Amberlite® IR-120, hyaluronidase (HYAL) from bovine testes, phosphate-buffered saline (PBS), and 2-mercaptoethanol (βME) were purchased from Sigma-Aldrich and used without further purification. Deuterium oxide (99.9%) was purchased from CortecNet and deionized water (conductivity

<0.1 μS) was prepared with an osmosis inverse system (Culligan). Filters (0.22 μm) were purchased from VWR. Lyophilized recombinant human Gal-3 was provided by Cell Guidance System (10 mM sodium phosphate, 50 mM sodium chloride, pH 7.5).

Synthesis procedure

Synthesis of LAC-NH_2

One equivalent of α-D-lactose was solubilized in a saturated 0.05 M NH_4OAc/EtOH solution, (18 mg/mL), at 40°C for about 30 min. 130 eq. of 28%–30% aqueous ammonia were added to the mixture, followed by the addition of three equivalents of $NaCNBH_3$. The reaction mixture was left under stirring at 90°C. After 8 h the solvent and the excess of ammonia were evaporated under reduced pressure to provide a white solid residue, which was washed with H_2O and EtOH. The crude product, solubilized in H_2O, was loaded onto an Amberlite IR-120 (H^+) column (20 equivalents of resin compared to amine) and eluted with deionized water until neutral pH to remove all the inorganic salts. During this step, the primary amine product remained anchored to the resin, and was liberated during elution with 50 mL of 10% aqueous ammonia solution and 50 mL of water. The products were detected using a TLC plate, with charring in 10% (v/v) sulfuric acid/EtOH. The collected product was then air-dried. The resulting residue was treated first with water and subsequently with EtOH until a constant weight was obtained to give a white solid product, with a yield of 90%.

Amidation with DMTMM

One equivalent of HA (nominal molecular weight of 90 and 400 kDa) was dissolved in deionized water at a concentration of 8 mg/mL. DMTMM (1–2.5 eq.) was added as a powder. To this solution, 1–2.5 eq. of a 1-amino-1-deoxy lactitol dissolved in water (40 mg/mL) was added (pH was measured and brought in a range of 6–7, when necessary, by addition of HCl 1 M solution). The reaction was stirred at room temperature for 48 h.[19] The entire reaction mixture was poured into isopropanol (up to a final concentration of 80% (isopropanol/H_2O 8/2, v/v). The white solid was recovered after centrifugation and washed several times with isopropanol. The product was further purified by either dialysis or ion-exchange. For the dialysis method, the crude product was dissolved in a minimal quantity of deionized water and dialyzed (Spectra/Por® 1 dialysis membrane, cut-off 6–8 kDa) in 0.1 M NaCl for 24 h, followed by 24 h in deionized water. The product was further concentrated to a small volume under reduced pressure and freeze-dried. In the ion-exchange resin method, after precipitation, the crude product was dissolved in deionized water (to a concentration of 10 mg/mL) and gently stirred with Amberlite IR-120 (H+) (30 equivalents of resin per amine) at room temperature for 30 min. The solution was then filtered through a glass-sintered funnel (porosity: G3), and the resulting solution was neutralized by addition of 5% $NaHCO_3$, concentrated and lyophilized.

General procedures of enzymatic hydrolysis

HA and HYLACH® samples were solubilized in deionized H_2O, at a concentration of 8 mg/mL, at 37°C and stirred until completely dissolved. HYAL (10 mg/ml in H_2O) was added for a final HYAL:HA ratio of 1:20 (w/w). To study the kinetics of hydrolysis, different timepoints (30′, 1, 2, 4, and 24 h) were considered. At prefixed timepoints, samples were taken and heated to 100°C for 15 s, to allow for HYAL denaturation, and filtered under vacuum (Filter c/o 0.22 μm) HYLACH oligomers (OHY) and HA oligomers (OHA) hydrolyzed sample solutions were freeze-dried for NMR, HP-SEC-TDA characterization and for molecular interaction analysis with Gal-3.

NMR spectroscopy

Proton NMR spectra were recorded at 313 K on a Bruker AVANCE NEO spectrometer operating at a proton frequency of 500 MHz (Bruker), equipped with 5 mm TCI cryoprobe. Carbon spectra were collected using a Bruker AVANCE IIIHD spectrometer operating at a proton frequency of 500 MHz (Bruker), equipped with 5 mm BBO probe, at 313 K. To achieve a final concentration of about 10 mg/mL for HA and HYLACH® samples and about 30 mg/mL for hydrolyzed products, dissolved in D_2O. The samples were stirred for at least 2 h to ensure complete solubilization, before being transferred to 5 mm NMR tubes (Bruker). ^{1}H-NMR were acquired with presaturation of residual HOD, using the Bruker zgcppr pulse program, with the following parameters: number of scans16, relaxation delay 12 s, time domain 32 k points and a spectral width of 18 ppm with transmitter offset 4.7 ppm. Heteronuclear single quantum correlation (HSQC) experiments were acquired using the Brucker hsqcedetgpsisp2.2 pulse program, with GARP4 decoupling. The following acquisition parameters were set: 32 number of scans, 16 dummy scans, relaxation delay 2 s, time domain 1 k, spectral width 10 ppm (F2) and 160 ppm (F1), transmitter offset 4.7 ppm (F2) and 90 ppm (F1), and number of *t1* increments equal to 320. The $^1J_{C-H}$ tune value was set to 150 Hz. Heteronuclear multiple bond correlation (HMBC) spectra were acquired using the Bruker hmbcetgpl2nd pulse program, with the following parameters: number of scans 32, dummy scan 2, relaxation delay 2 s, time domain 2 K and number of *t1* increments equal to 256, with a long-range coupling of 8 Hz, spectral width 10 ppm (F2) and 160 ppm (F1), transmitter offset 4.7 ppm (F2) and 90 ppm (F1). HSQC–distortion enhancement by polarization transfer (multiplicity-edited HSQC) were acquired using Bruker hsqcedetgpsisp2.2 pulse program, with the following parameters: number of scans 48, dummy scan 16, relaxation delay 2 s, time domain points 2 K, spectral width 10 ppm (F2) and 160 ppm (F1), transmitter offset 4.7 ppm (F2) and 90 ppm (F1). HSQC and HMBC spectra were acquired using the phase-sensitive mode, by using the time-proportional phase incrementation.

COSY spectra were acquired using the Bruker cosygpprqf pulse program with water presaturation, with the following parameters: number of scans 20, relaxation times 2 s, time domain 20 k, *t1* increments 256, and spectral width 10 ppm (F2) and 10 ppm (F1), with transmitter offset 4.7 ppm. The TOCSY spectra were acquire with Brucker mlevphpr pulse program, with the following parameters: number of scans 20, relaxation times 2 s, time domain 20 k, mixing time 80 ms, spectral width 10 ppm (F2) and 10 ppm (F1), with transmitter offset 4.7 ppm.^{13}C spectra were acquired with Bruker pulse sequence zgig, with the following parameters: number of scans 24 k, dummy scans 4, relaxation delay 2 s, time domain 33 k, and a spectral window of 300 ppm, transmitter offset 90 ppm. Spectra were processed with Bruker Topspin Software 4.1.1.

HP-SEC-TDA

The molecular weight distributions were determined by HP-SEC-TDA, widely used for the analysis of polymers,[20,21] without column calibration. Chromatographic acquisitions were performed on a Viscotek system model TDA305 (Malvern Panalytical) equipped with a multidetector system (refractive index [RI], right and low angle light scattering, and viscometer [DP]). Sample solutions were obtained solubilizing 20–25 mg in a suitable volume of mobile phase and mixing for 3 h. HA or HYLACH® were analyzed at a concentration of ~0.5 mg/mL, while hydrolyzed products were at a concentration of ~4 mg/mL. Measurements were performed at 40°C, at a flow rate of 0.6 mL/min, using 2 × TSKGMPWXL columns 13 µm. 7 mm ID × 30 cm L, in series (Tosoh Bioscience). A solution of 0.1 M $NaNO_3$ containing 0.05% of NaN_3, prefiltered using a 0.22 µm filter (Millipore Merck) was used as mobile phase. The detectors were calibrated with Pullulan standard, with molecular weight, polydispersity index, and intrinsic viscosity (η) certified (PolyCAL-PullulanSTD-Malvern Panalytical). Chromatographic profiles were elaborated using OmniSEC software version 4.6.2. For all the samples the RI increment (dn/dc) of 0.155, known in literature for HA, was used.[22]

Electrospray ionization mass spectroscopy (ESI-MS)

Direct infusion ESI-MS analysis, of LAC-NH_2, was performed on an Impact II ESI-Q-TOF mass spectrometer (Bruker Daltonics). The spectrum was acquired in positive ion mode (capillary voltage −4.5 kV) in the *m/z* 50–1300 mass range. Nitrogen was used as a drying (4 L/min) and nebulizing gas (0.4 bar) and the ion transfer capillary was kept at 200°C.

Isothermal titration calorimeter (ITC)

Biomolecular interactions were determined by ITC analyses, performed on a MicroCal PEAQ-ITC (Malvern Panalytical), equipped with MicroCal PEAQ-ITC Analysis Software. Gal-3 protein was reconstituted in a solution of PBS and β-mercaptoethanol at a concentration of 10 µM. Ligand solution of LAC-NH_2, galactose, lactose, HA, and HYLACH® oligomers (labeled OHA and OHY, respectively) were solubilized in PBS buffer at different concentrations (between 295 and 400 µM). ITC experiments were carried out at 25°C. Two hundred micrometer of protein solution were loaded on the sample cell, while each ligand solution was loaded in the syringe. Two microliter of ligand were injected 20 times, with a delay of 60 and 150 s between injections, and the stirring rate set to 500 rpm. For each ligand injection, the measured heat released upon complex formation was fitted to a single binding site model using the following equation:

$$Q(i) = \frac{nP_t\Delta HV\left\{1 + \frac{X_t}{nP_t} + \frac{1}{nKP_t} - \left[\left(1 + \frac{X_t}{nP_t} + \frac{1}{nKP_t}\right)^2 - \frac{4X_t}{nP_t}\right]^{\frac{1}{2}}\right\}}{2}, \quad (1)$$

where $Q(i)$ is the heat corresponding to the *i*th injection, V is sample cell volume; ΔH is the enthalpy; $[P_t]$ is the cell protein concentration; $[X_t]$ is the syringe ligand concentration, n is the number of binding sites, and K is the binding constant.

To estimate the thermodynamic parameters (K_D, ΔH, and ΔS), the data were fitted using MicroCal analysis software using the "one set of sites" interaction model. Blank experiments on the free ligands diluted in PBS and β-mercaptoethanol were recorded and the measured heat subtracted from the reaction heat data.

CD spectroscopy

CD analyses were performed on a J1500 Circular Dichroism Spectrophotometer (Jasco) and raw data were elaborated with Jasco Spectra Manager Software. Gal-3 protein was prepared as indicated in the ITC experimental method section at a final concentration of 10 µM, and 200 µL were employed for every ligand tested (lactose, LAC-NH_2 and oligomers of HA (OHA), HYLACH® 1, and HYLACH® 2). Ligand stock solutions were solubilized in PBS to obtain 2.94 mM concentration. CD spectra were collected at 25°C and recorded using a quartz cell (Hellma UK), with a path length of 1 mm, response time of 1 s, scan speed of 20 nm/min, and bandwidth of 0.5 nm, and each spectrum was built from the average of three scans. For each CD measurement, a titration of the ligand into the protein was performed. Far CD-UV spectra (200–250 nm) were recorded for at least 11 ligand/protein molar ratios (L/P), in the range 0–8. Spectra of the free ligands were recorded under the same conditions as the blank, and the CD signals were subtracted from the protein–ligand complex signals.

RESULTS AND DISCUSSION

LAC-NH_2 synthesis and characterization

1-amino-1-deoxy lactitol, or LAC-NH_2, was prepared by the reductive amination of lactose, employing the metal hydride-/ammonia-mediated reductive amination of hemiacetals.[19] The

protection-group-free synthesis of primary amine favors a one-step chemoselective preparation of primary amine LAC-NH_2, as described in Scheme 1. The structure of the product was confirmed by homonuclear and heteronuclear NMR experiments (Supporting Information S1: Figure S1 and Table S2) and the complete proton and carbon signal assignments are in agreement with the literature.[23] Further confirmation of the synthesized LAC-NH_2 structure was obtained using mass spectroscopy that shows the presence of a peak at m/z 344 ($M+H^+$), corresponding to the molecular weight of LAC-NH_2 ($C_{12}H_{25}NO_{10}$). Data not shown.

HYLACH® synthesis

HYLACH® was obtained by reaction between HA and LAC-NH_2, where the amino-lactose derivative is covalently conjugated to the HA. This reaction results in the formation of an amide bond between carboxylic groups of the GlcA residue of HA and amine of LAC-NH_2, as illustrated in Scheme 2. The synthesis has been performed to obtain compounds with a DS between 10% and 40%, which were found to provide better results in preliminary in silico studies.[8] The syntheses were performed in aqueous media, in the presence of a commercially available condensing agent (CA), DMTMM,[24] known to be highly soluble and stable in water for an extended period of time.[25] This allows the formation of an ammonium salt of DMTMM which reacts, by a substitution mechanism, with the carboxylic group of HA to form the active triazine-ester followed by a nucleophilic attack of LAC-NH_2.[7]

To synthesize samples with different DS values in a range considered ideal according to previous biological evaluation,[8] various reaction parameters, such as stoichiometry of the triazine condenser (DMTMM) and LAC-NH_2, and pH, were optimized. Reactions were carried out on both the nominal molecular weight 90 and 400 kDa HA, at different scales, from mg to g. A summary of the reaction conditions is reported in Table 1. HYLACH® samples were obtained, in quantitative yield, after a purification step involving precipitation in isopropanol (80%), performed following dialysis or ion exchange as described in Section 2.2.2. No significant difference between ion exchange and dialysis methods was observed.

HYLACH® characterization

NMR spectroscopy

HYLACH® products were characterized by NMR spectroscopy with monodimensional (^1H,^{13}C), bidimensional homonuclear (COSY, Supporting Information S1: Figure S3) techniques, and heteronuclear 2D experiments (multiplicity-edited HSQC, HMBC). HYLACH® ^1H-NMR spectra confirmed the addition of peaks concerning LAC-NH_2, however, no significant chemical shift changes were observed following functionalization. Through bidimensional experiments, all the peaks were attributed, and the formation of the amide bond was confirmed by HMBC experiments (Supporting Information S1: Figure S4). Figure 1 shows a typical ^1H-^{13}C HSQC spectrum of HYLACH®, while its chemical shift values are listed in Table 2.

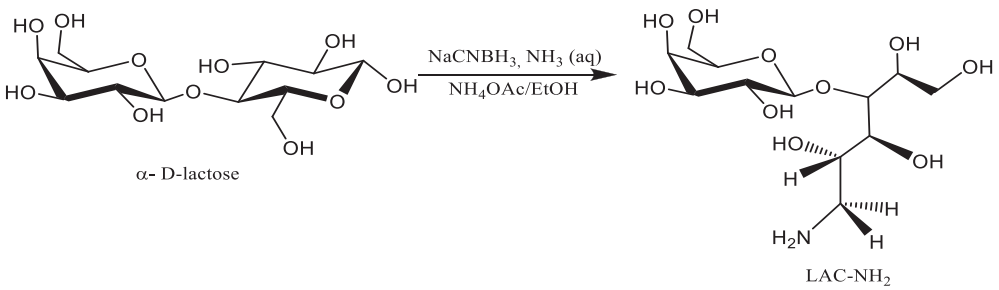

SCHEME 1 Synthesis of 1-amino-1-deoxy-lactitol (LAC-NH_2).

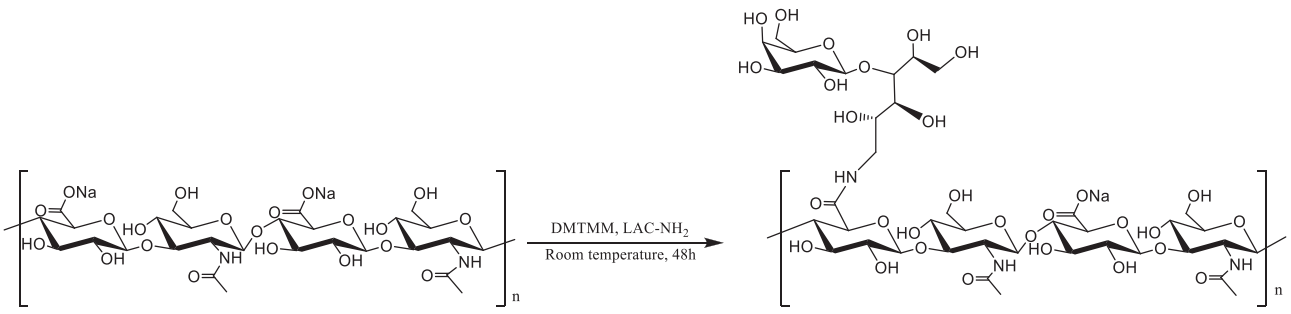

SCHEME 2 Synthesis of HYLACH®. LAC-NH_2, 1-amino-1-deoxy-lactitol.

Determination of the DS

The literature reports that ^{1}H NMR spectra are usually used to evaluate the DS of functionalized HA, integrating ligand signals with respect to the CH_3 groups of GlcNAc.[26,27] Owing to the complexity of the ^{1}H NMR spectra of our samples and the absence of a clear and well resolved proton signal of LAC-NH_2, this method could not be applied to HYLACH®. In HSQC experiments, the presence of a well-defined CH signal of S2 of LAC-NH_2 separated from the other signals of the backbone, was observed. Since in the literature, quantitative 2D-HSQC analysis applied to different polysaccharides such as sulodexide,[28] heparin,[29] and pentosan polysulfate[20] are reported, the determination of DS of HYLACH® through 2D NMR spectra was attempted. The huge differences in molecular size and mobility between the backbone of polysaccharide and the pendant disaccharide, however, led to different longitudinal relaxation time (T_1) and transverse relaxation times (T_2), especially for ^{13}C nuclei, influencing the integral measurements and subsequent results. This behavior is more evident for HYLACH® compounds obtained from HA of 400 kDa, where DS values higher than 100%, determined by 2D NMR, were found. To overcome this problem, enzymatic depolymerization of the polysaccharide was introduced to reduce molecular weight without affecting the substitution and consequently the motional behavior difference between the OHA and the amino-lactose branching. Hydrolysis of HA and HYLACH® derivatives were performed with HYAL type I.[30,31] The mechanism of depolymerization involves the cleavage of β 1 → 4 glycosidic bonds, leaving intact the amide bond with LAC-NH_2. As reported in the literature,[32] selective HA hydrolysis to the constituent disaccharides is challenging; in our case, after 24 h of depolymerization, OHA showed a Mw of approximately 5 kDa and between 6 and 14 kDa for HYLACH® oligomers. Distinct from HYLACH®, the HSQC spectrum of hydrolyzed HYLACH® oligomers (Figure 2) exhibits the presence of reduced anomeric signals attributed to reducing end GlcNAc H1α and GlacNAc H1β (indicated as *A*1*α* − *r* and *A*1*β* − *r*), as well as reducing GlcNAcm − *r* and *A*2*β* − *r*) compared to starting HYLACH®. The DS, expressed as the percentage of substituent compared to HA disaccharide repetitive units, was obtained according to the following formula:

TABLE 1 Reaction conditions for the preparation of HYLACH®.

HYLACH® sample	Starting HA (Mw, kDa)	Reaction conditions		
		LAC-NH_2 (eq.)	DMTMM (eq.)	pH
HYLACH® 1	90	0.5	0.5	≈7
HYLACH® 2	90	1.5	1.5	≈7
HYLACH® 3	90	1.5	1.5	>8
HYLACH® 4	400	1.5	1.5	>8
HYLACH® 5	400	2.5	2.5	≈7

Abbreviations: DMTMM, 4-(4,6-dimethoxy-1,3,5-triazin-2-yl)-4methyl morpholinium chloride; HA, sodium hyaluronate; LAC-NH_2, 1-amino-1-deoxy-lactitol; Mw, wieght-average molecular weight.

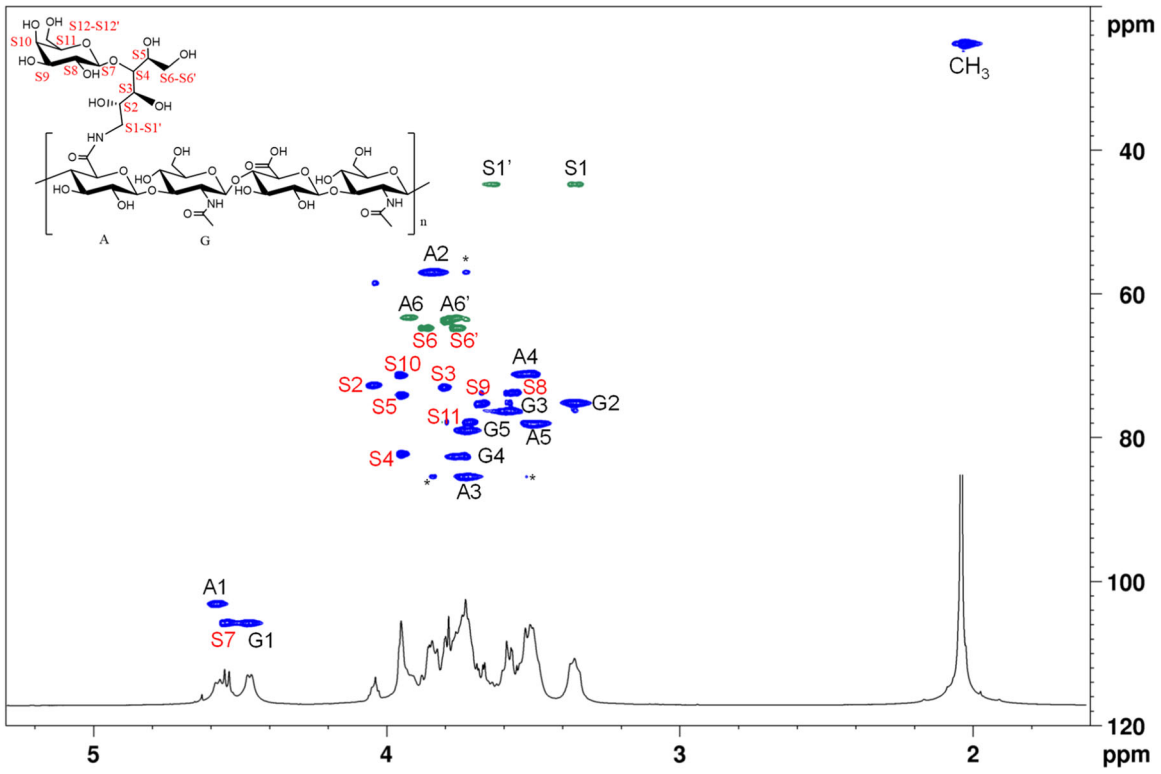

FIGURE 1 Assignment of HYLACH® ^{1}H and ^{13}C NMR signals. Superimposition of ^{1}H-^{13}C HYLACH® HSQC-edited (CH_2 are reported in green and CH and CH_3 signals in blue) and ^{1}H spectrum.

TABLE 2 Full assignment of NMR signals (^{1}H,^{13}C) of functionalized HA (HYLACH®).

Assignment	^{1}H (ppm)	^{13}C (ppm)
Ac (CH_3)	2.03	25.2
A1	4.57	103.2
A2	3.84	57.1
A3	3.72	85.5
A4	3.52	71.2
A5	3.50	78.2
A6	3.92	63.4
A6′	3.77	63.4
G1	4.47	105.8
G2	3.35	75.2
G3	3.58	76.4
G4	3.74	82.7
G5	3.73	79.1
S1	3.36	44.8
S1′	3.62	44.8
S2	4.04	72.7
S3	3.80	73.1
S4	3.95	82.4
S5	3.94	74.1
S6	3.86	64.8
S6′	3.76	64.8
S7	4.54	105.8
S8	3.57	73.9
S9	3.68	75.4
S10	3.95	71.3
S11	3.72	78.0
S12–S12′	3.79	63.8
CONH	-	172.3
COO^-	-	176.8
Ac (CO)	-	177.7

Abbreviation: HA, sodium hyaluronate.

$$DS = \frac{(S2)}{(A2 + A2\beta - r. + A2\alpha - r)}100\%. \quad (2)$$

Where S2 integral value, shown in Figure 2, is divided by the sum of *A2* and *A2* (reducing end) signals.

Investigation of the correlation between Mw and DS during a kinetic hydrolysis, led to DS being properly estimated through quantitative 2D-HSQC spectra, when the HYLACH® oligomers were in a Mw range between 6 and 20 kDa. DS values obtained as a function of the stoichiometry ratio of reagent and pH, were in the range between 14% and 44% for all the synthetized HYLACH® (Table 3). An increase of LAC-NH_2 compared to HA leads to higher DS values, HYLACH® **1** (0.5 eq.; DS = 14%) toward HYLACH® **2** (1.5 eq.; DS = 37%), while a pH higher than 8, leads to lower DS as observed for HYLACH® **3** (23%) compared to HYLACH® **2** (DS: 37%). Analogous results were obtained for HYLACH® **4**, DS 18% and HYLACH® **5**, 2.5 eq., DS: 44%, obtained under different reactions conditions.

Molecular weight distribution

The chromatographic profiles of 90 and 400 kDa HA, overlapped with their derivatives (HYLACH® 1 and HYLACH® 4, respectively), are shown in Figure 3A,B, respectively. The samples had an elution volume between 12 and 16 mL, with a broad bell-shape chromatographic peak, caused by a high polydispersion index. Weight-average molecular weight (Mw), number-average molecular weight (Mn), and molecular-weight dispersity (Mw/Mn) values are reported in Table 3. In addition, values of hydrodynamic radius (Rh), η value, value of a and logK, corresponding, respectively, to the slope and intercept constants of the Mark–Houwink curve derived from HP-SEC-TDA, are also reported. All the results refer to the mean values of duplicate injections. HP-SEC-TDA profiles showed that HYLACH® at 400 kDa leads to partial hydrolysis of HA, not observed for the 90 kDa HA. On the other hand, the result of a blank experiment obtained using 400 KDa HA in the presence of DMTMM, and left stirred for 48 h, revealed a reduction in Mw of HA of the same order of magnitude as HYLACH® samples (Supporting Information S1: Figure S5 and Table S6). Interestingly, this phenomenon was not observed in the absence of CA. The Mw/Mn remains constant and similar to the starting HA, thus indicating that there is no increase in polydispersity after the functionalization of the HA. The Rh for HYLACH® samples obtained from 90 kDa HA remains constant, while this value decreases for HYLACH® samples obtained from 400 kDa HA, due to the partial depolymerization occurring during the polymer derivatization. The η of HA is influenced by the Mw, as observed for the comparison of η values of 400 and 90 kDa HA. This behavior does not occur for HYLACH® samples, in fact, η values decrease with increasing Mw, possibly indicating that modification of the structure (different DS) induces different rheological properties. This variation could indicate a difference in intra- or intermolecular interactions,[33] which alters the chemical properties of the polymers (manuscript in preparation). This phenomenon is also observed for HYLACH® at high molecular weight, despite the fact that depolymerization occurred during the functionalization reactions. *logK* and *a* have similar values and of the same order as data reported in the literature,[34] in addition, "a" values are in the range of 0.7–0.9, thus indicating that, regardless of Mw and DS, the molecules remain in a random coil conformation. The weight recovery, determined by the RI area, is in a range between 81% and 94% for all the samples injected and this value is compatible with the water absorption by dry samples.

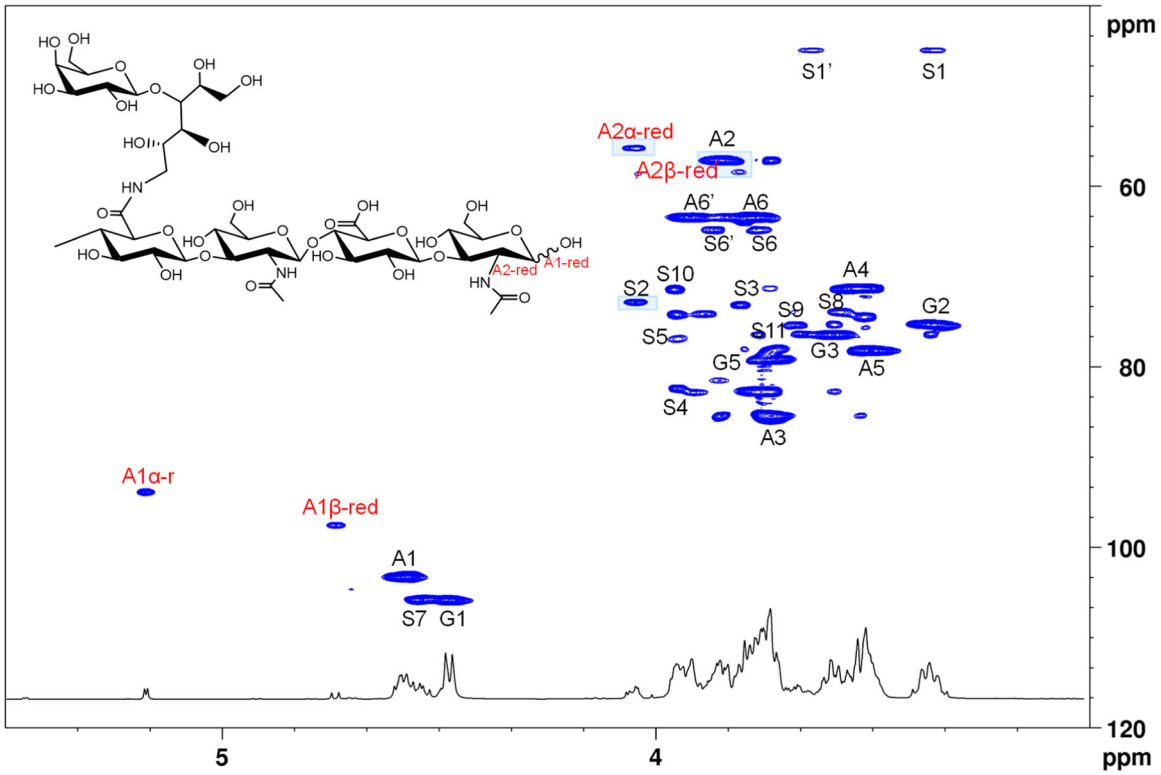

FIGURE 2 Two-dimenisonal NMR spectroscopy for the determination of the degree of substitution. Superimposition of ^{1}H-^{13}C heteronuclear single quantum correlation and ^{1}H spectra of hydrolyzed HYLACH® sample. The signals integrated for the calculation of the degree of substitution are highlighted in light blue.

TABLE 3 Results of HP-SEC-TDA analysis.

Samples	Starting HA nominal Mw (kDa)	DS%	Mw (kDa)	Mn (kDa)	Mw/Mn	Rh (nm)	η (dL/g)	a	logK
90 kDa HA	-	-	82	58	1.4	14	2.4	0.88	−3.9
HYLACH® 1	90	14	86	66	1.4	14	2.2	0.85	−3.9
HYLACH® 2	90	37	95	68	1.5	13	1.6	0.79	−3.7
HYLACH® 3	90	23	89	63	1.5	14	2.0	0.78	−3.5
400 kDa HA	-	-	325	209	1.5	33	7.5	0.76	−3.3
HYLACH® 4	400	18	260	170	1.5	27	5.5	0.80	−3.6
HYLACH® 5	400	44	280	174	1.6	25	3.9	0.77	−3.6

Note: DS (%) determined by formula 1.

Abbreviations: *a* and logK, Mark–Houwink costant; DS, degree of substitution; HA, sodium hyaluronate; HP-SEC-TDA, high-performance size exclusion chromatography with triple detector array; Mn, number-average molecular weight; Mn/Mw, molecular-weight dispersity; Mw, weight-average molecular weight; Rh, hydrodynamic radius; η, viscosity.

HYLACH® stability toward HYAL

The hydrolysis procedure, for the determination of DS, allows the determination of HYLACH® stability toward HYAL depolymerization. Hydrolysis curves over time are shown in Figure 4.

From the hydrolysis curves, it is evident that 90 kDa HA presents a lower degree of enzymatic depolymerization than to 400 kDa HA. On the other hand, all HYLACH® samples, exhibited a degree of depolymerization lower than native HA, and inversely proportional to the DS (see Table 3).

Isothermal titration microcalorimetry

ITC experiments were performed to address the interaction between Gal-3 and HA or HYLACH®. This sensitive technique measures the

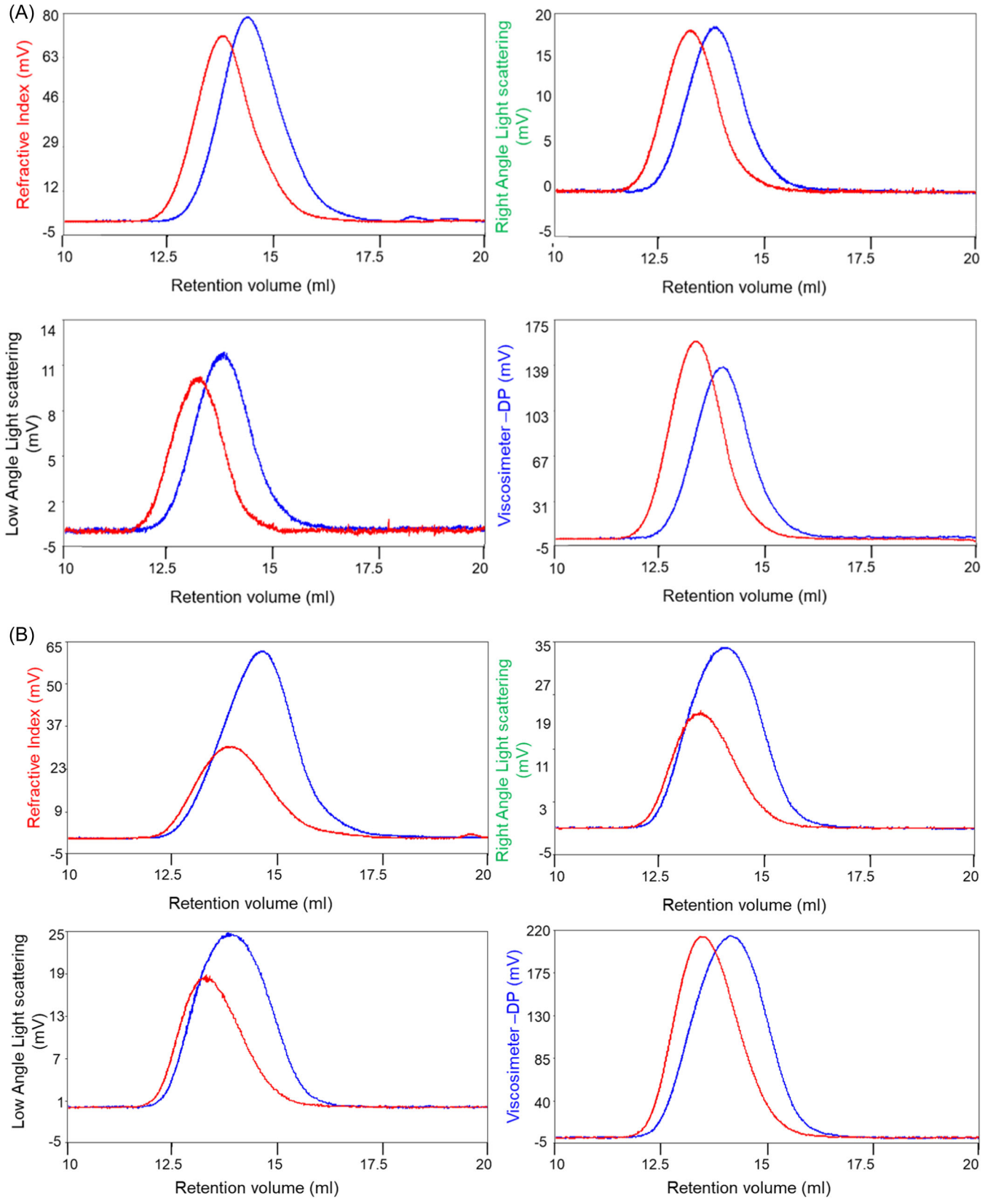

FIGURE 3 Determination of molecular weight high-performance size exclusion chromatography with triple detector array profiles with refractive index, viscometer, right and low angle light scattering of (A) 400 kDa sodium hyaluronate (HA) (red) and HYLACH®4 (blue) and (B) 90 kDa HA (red) and HYLACH®1 (blue).

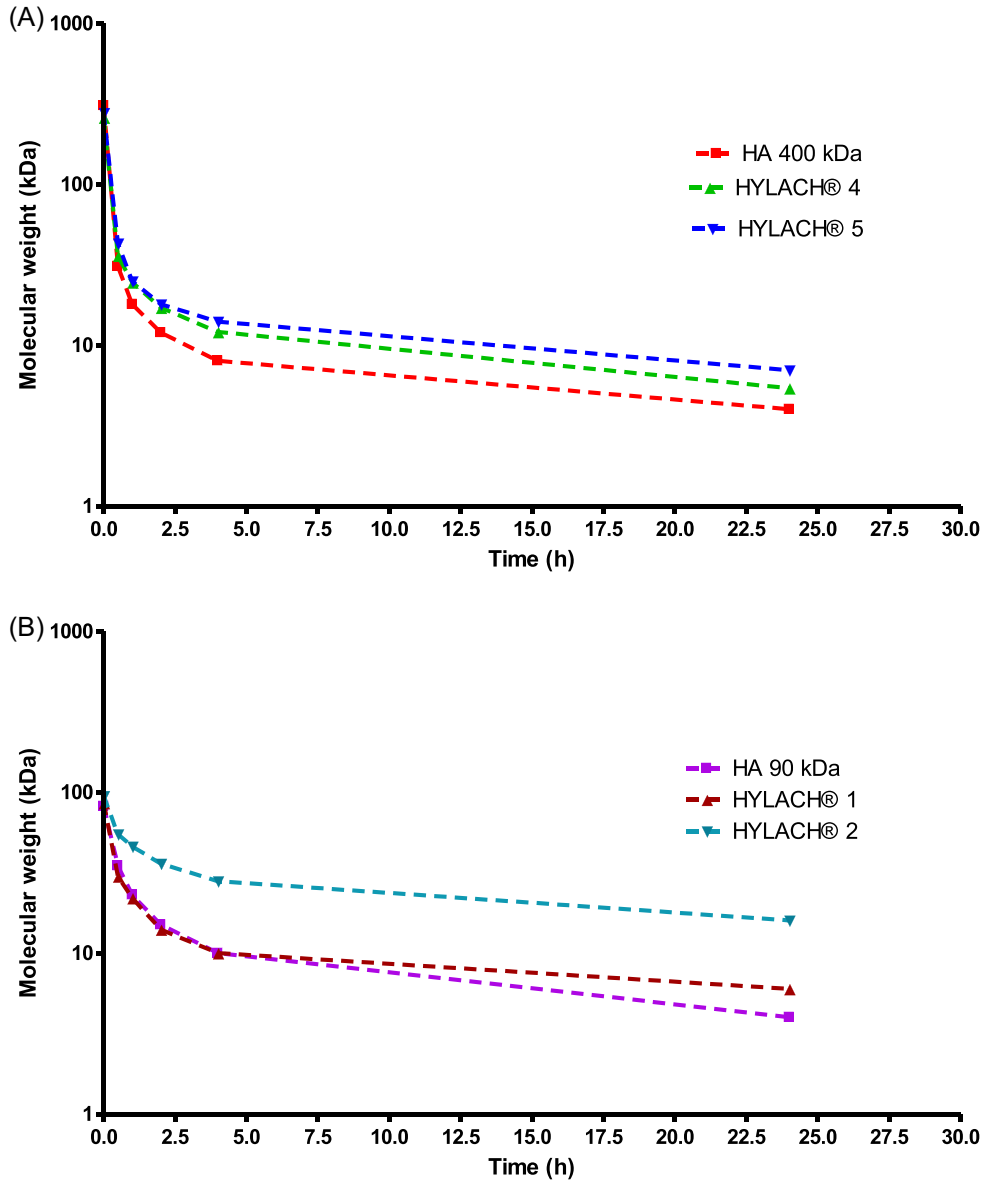

FIGURE 4 Investigation of HYLACH® enzymatic stability. Hydrolysis curves over time of; (A) 400 kDa sodium hyaluronate (HA) and its corresponding HYLACH® samples (B) 90 kDa HA and its corresponding HYLACH® samples.

differential power, applied to the cell heaters, required to minimize the temperature difference between the reference and the sample cell. In addition, ITC has the advantages that it does not require labeling or immobilization of the ligands and can be performed in solution. The thermodynamic parameters obtained, such as the stoichiometry (N), dissociation constant (K_D), variation of enthalpy (ΔH), variation of Gibbs free energy (ΔG), and variation of entropy ($T\Delta S$), are reported in Table 4. Interaction studies were performed on saccharide ligands and OHA and HYLACH® (OHY1 and OHY2), obtained by enzymatical hydrolysis. OHY1 and OHY2 were selected due to the similarity of molecular weight and DS with HYLACH 1 and HYLACH 3, respectively, cited by Donato et al.[8]

ITC results showed that the interactions between Gal-3 and saccharide ligands, OHA and OHY are all energetically favorable binding reactions (ΔG negative) and entropically driven ($T\Delta S > 0$), except for OHY2. For small ligands (LAC-NH_2, galactose, and lactose) the stoichiometry of the interaction (N) is in the order of 1 protein:1 ligand, and the dissociation constant (K_D) is the order of μM, with values similar to data reported for lactose.[35–40] On the other hand, strong binding is also obtained for galactose compared to that previously determined, and this could be due to the low protein concentration used in the ITC experiments. The relative affinities, however, showed the same trend, and the LAC-NH_2 and lactose results showed slightly higher interaction with Gal-3 than galactose. To evaluate the influence of variation of Mw on protein interaction, OHA were studied at two molecular weights of about 8 and 22 kDa. No significant difference in thermodynamic parameters of the binding was observed, suggesting that there was little variation with

TABLE 4 Thermodynamic parameters obtained by isothermal calorimetry for the interaction of test compounds with galectin-3.

Sample	Mw (Da) (DS%)	*N* (sites)	K_D (μM)	Δ*H* (kcal/mol)	Δ*G* (kcal/mol)	*TΔS* (kcal/mol)
LAC-NH_2	380	0.97 ± 0.12	9.24 ± 1.79	−4.49 ± 0.83	−6.87	2.38
Galactose	180	1.29 ± 0.17	19.7 ± 3.46	−3.06 ± 0.63	−6.42	3.36
Lactose	340	1.37 ± 0.13	13.4 ± 2.41	−2.7 ± 0.43	−6.66	3.96
OHA	22,000	0.59 ± 0.03	1.55 ± 0.27	−0.22 ± 0.02	−7.93	7.71
OHA	8000	0.73 ± 0.02	1.36 ± 0.16	−0.14 ± 0.05	−8.00	7.86
OHY1	6000 (14%)	0.72 ± 0.04	1.91 ± 0.35	−0.18 ± 0.01	−7.81	7.63
OHY2	14,000 (37%)	0.85 ± 0.12	9.13 ± 1.63	−9.83 ± 1.87	−6.88	−2.95

Abbreviations: [L], Ligand concentration; DS, degree of substitution express in %; KD, dissociation constant; Mw, molecular weight; *N*, number of sites; OHA, sodium hyaluronate oligomers; OHY, HYLACH® oligomers; −*TΔS*, variation of entropy; Δ*G*, variation of Gibbs free energy; Δ*H*, variation of enthalpy.

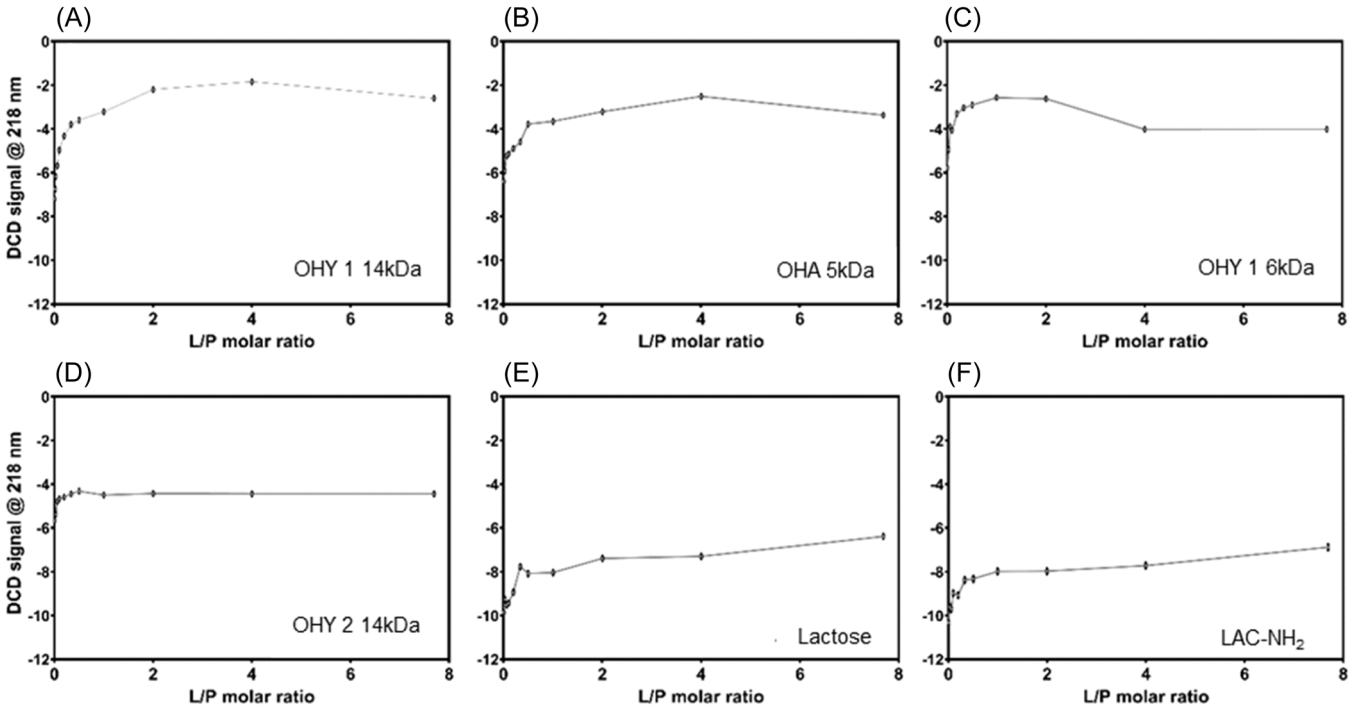

FIGURE 5 Circular dichroism plots to evaluate protein conformation variation upon ligand binding. Circular dichroism (CD) signal variations at 218 nm, the maximum (negative) CD ellipticity for Galectin-3 (Gal-3) in the apo form, monitored in titration spectra of Gal-3 in the presence of increasing concentrations of sodium hyaluronate (HA) and HYLACH® oligomers (HA oligomers [OHA] and HYLACH oligomers [OHY], respectively) obtained after enzymatical hydrolysis compared to Lactose and 1-amino-1-deoxy-lactitol (LAC-NH_2). In details in figure are reported: (A) OHY®1 (molecular weight: 6 kDa, degree of substitution: 14%), (B) OHA (molecular weight: 5 kDa), (C) OHY1 oligomer (molecular weight: 14 kDa, degree of substitution: 14%) (D) OHY2 oligomer (molecular weight: 14 kDa, degree of substitution: 37%), (E) lactose, and (F) LAC-NH_2.

the molecular weight. Thermodynamic parameters revealed that the binding of HA to Gal-3 is characterized by hydrogen bonding and hydrophobic interactions as indicated by the higher favorable entropy contribution ($\Delta S > 0$). Similar binding affinity in the micro-molar range and thermodynamic parameters were obtained in the binding of HYLACH® oligomers at lower DS (OHY1). For both OHA and OHY the number of sites (*N*) is around 0.7, which means that one ligand is bound to two proteins, suggesting that full-length (recombinant) human Gal-3 protein might dimerize upon oligomer binding, as previously reported for multivalent carbohydrates that induce the self-association of Gal-3.[41,42] Interestingly, the binding of OHY2 with higher DS (37%) showed a different feature, as indicated by the enthalpic gain that appears to compensate for the loss in entropy, ($\Delta H < 0$ and $\Delta S < 0$), and that can be ascribed to: (i) restriction of the conformational freedom of the functionalized HYLACH® ligand upon binding; (ii) protein conformational rearrangements upon

ligand binding; (iii) reorganization of water molecules solvating the protein and/or the ligand. It is possible to speculate that in HYLACH® the pendant LAC-NH_2, although not changing the conformation of the HA-derived backbone, stiffens the overall structure which can, as a consequence, partially impair the wrapping around the Gal-3 molecule. It should also be considered that in HYLACH® fewer negative charges are available in comparison to HA. This is the consequence of the covalent binding of LAC-NH_2 to glucuronic acid units of the backbone. As for many proteins at neutral pH, Gal-3 possesses a positive electrostatic potential with a pI of 8.58 (as estimated by ExPASy-ProtParam prediction server using the primary protein structure as a template). Structural analysis highlighted the presence of a positively charged "belt" spanning around the protein surface, compatible with the binding to a linear negatively charged polymer. The possible increase in rigidity combined with fewer available negative charges may decrease the electrostatic interactions and increase the specificity of HYLACH® binding. In addition, HYLACH® (OHY1 and OHY2), but not HA, have been reported to provide anti-inflammatory properties in an in vitro inflammation model of lung fibroblasts as showed by Donato et al.[8] This is likely to be the consequence that although with the same affinity of HA, the specific occupation of the CRD pocket by LAC-NH_2, triggers Gal-3 function in reduction of both gene and protein expression of fundamental profibrotic molecules as reported by Donato et al.[18]

CD

CD measurements were performed to address conformational changes of Gal-3 upon ligand binding. Specifically, the CD signal in the far-UV (200–250 nm) provides information concerning possible changes in the protein secondary structure and conformation (α-helices, β-sheet, and unstructured regions) that may be induced by interactions with other ligands. In the CD analysis, no significant variation of protein secondary structure content was observed, however, a decrease in the intrinsic CD signal was observed when titrating increasing concentrations of OHA and OHY ligands, reflecting the destabilizing and/or oligomerization of the protein (Supporting Information S1: Figure S7 and Table S8). In more detail, the intensity at 218 nm, where the CD signal change was more significant, was plotted versus the Ligand/Protein molar ratio. Interestingly, in OHA and OHY, (Figure 5A–D) the maximum in CD signal variation was reached at an L/P molar ratio of 0.5, and this is in line with ITC data, in which one molecule of ligand is bound to two molecules of Gal-3. Interestingly, the interaction of the protein with OHY2 at higher DS (37%) resulted in small CD signal variations comparable to the LAC-NH_2 and lactose (Figure 5E,F), suggesting lower affinity and destabilization of the protein. The CD data on the reference small ligands, however, showed that the maximum variation of CD signal was reached in both cases at L/P molar ratio of 1, which is in good agreement with the stoichiometry measured by ITC data.

CONCLUSION

In this paper, we reported the synthesis and characterization of a new biopolymer, denoted as HYLACH®, by functionalization of HA with LAC-NH_2. The molecular weight distribution of HYLACH®, determined by HP-SEC-TDA, was in the range of 85 to 290 kDa depending on the starting HA. The products were structurally characterized and the DS, determined by a validated bidimensional NMR method on the hydrolyzed samples, was found between 14% to 44% depending on the synthetic condition used. The introduction of a hydrolysis step was necessary to determine the DS by 2D-NMR, not directly measurable on high molecular weight polysaccharides. ITC experiments provided that HYLACH® oligomers present strong affinities for Gal-3 in μM range, and this is consistent with literature of the enhancing of binding affinity for larger oligosaccharides, as well as complex-type *N*-glycans and poly-*N*-acetyllactosamine.[43–45]

CD experiments agreed with ITC data. Despite little variation of protein secondary structure being observed, a reduction in CD signals was seen with interaction studies of HYLACH® and OHA. It was also observed that ligand binding significantly affected the stability of Gal-3, suggesting a further investigation of these functionalized HA as therapeutic inhibitors of Gal-3 associated human diseases such as the treatment of pulmonary disease and IPF. Our results show how the combination of safety and biocompatibility of a functionalized HA able to bind Gal-3 opens-up new perspectives in the therapy of IPF and the results suggest that HYLACH® can be further investigated as a specific potential therapeutic drug.

AUTHOR CONTRIBUTIONS

Sofia Nizzolo: Investigation; methodology; conceptualization; writing—original draft; writing—review and editing. **Emiliano Esposito**: Conceptualization; investigation; writing—original draft; writing—review and editing. **Ming-Hong Ni**: Investigation; writing—original draft; writing—review and editing. **Laura Bertocchi**: Writing—review and editing. **Giulio Bianchini**: Conceptualization; writing—review and editing. **Nadia Freato**: Writing—review and editing. **Serena Zanzoni**: Investigation; writing—original draft; writing—review and editing. **Marco Guerrini**: Conceptualization; writing—review and editing. **Sabrina Bertini**: Conceptualization; project administration; supervision; writing—review and editing.

ACKNOWLEDGMENTS

We would like to acknowledge Dr. Yates (University of Liverpool) for the discussion and editing of the final paper, Cosentino and Dr. Savino (Ronzoni Institute) for NMR characterization, Dr. Naggi for the consultation about the project, and Dr. Elli (Ronzoni Institute) for the interesting discussion about conformational properties of HYLACH®. S. N., E. E., M.-H. N., M. G., and S. B. were supported by the Non-Profit Research Foundation "Istituto di Ricerche Chimiche e Biochimiche G. Ronzoni."

CONFLICT OF INTEREST STATEMENT

The authors declare no conflict of interest.

DATA AVAILABILITY STATEMENT

The data that support the findings of this study are available from the corresponding author upon reasonable request.

ETHICS STATEMENT

The authors confirm that the ethical policies of the journal, as noted on the journal's author guidelines, have been adhered to.

REFERENCES

[1] N. M. Salwowska, K. A. Bebenek, D. A. Żądło, D. L. Wcisło-Dziadecka, *J. Cosmet. Dermatol.* **2016**, *15*, 520.
[2] C. Buckley, E. J. Murphy, T. R. Montgomery, I. Major, *Polymers* **2022**, *14*, 3442.
[3] J. R. Fraser, T. C. Laurent, U. B. Laurent, *J. Intern. Med.* **1997**, *242*, 27.
[4] L. W. Moreland, *Arthritis Res. Ther.* **2003**, *5*, 54.
[5] M. Dovedytis, Z. J. Liu, S. Bartlett, *Eng. Regen.* **2020**, *1*, 102.
[6] S. Vasvani, P. Kulkarni, D. Rawtani, *Int. J. Biol. Macromol.* **2020**, *151*, 1012.
[7] C. E. Schanté, G. Zuber, C. Herlin, T. F. Vandamme, *Carbohydr. Polym.* **2011**, *85*, 469.
[8] A. Donato, F. Fontana, R. Venerando, A. Di Stefano, P. Brun, *Polymers* **2023**, *15*, 1616.
[9] P. Spagnolo, J. A. Kropski, M. G. Jones, J. S. Lee, G. Rossi, T. Karampitsakos, T. M. Maher, A. Tzouvelekis, C. J. Ryerson, *Pharmacol. Ther.* **2021**, *222*, 107798.
[10] S. Barratt, A. Creamer, C. Hayton, N. Chaudhuri, *J. Clin. Med.* **2018**, *7*, 201.
[11] L. Li, J. Li, J. Gao, *J. Pharmacol. Exp. Ther.* **2014**, *351*, 336.
[12] R. J. Slack, R. Mills, A. C. Mackinnon, *Int. J. Biochem. Cell. Biol.* **2021**, *130*, 105881.
[13] K. V. Mariño, A. J. Cagnoni, D. O. Croci, G. A. Rabinovich, *Nat. Rev. Drug Discov.* **2023**, *22*, 295.
[14] S. Sciacchitano, L. Lavra, A. Morgante, A. Ulivieri, F. Magi, G. De Francesco, C. Bellotti, L. Salehi, A. Ricci, *Int. J. Mol. Sci.* **2018**, *19*, 379.
[15] Y. Nishi, H. Sano, T. Kawashima, T. Okada, T. Kuroda, K. Kikkawa, S. Kawashima, M. Tanabe, T. Goto, Y. Matsuzawa, R. Matsumura, H. Tomioka, F. T. Liu, K. Shirai, *Allergol. Int.* **2007**, *56*, 57.
[16] A. C. MacKinnon, M. A. Gibbons, S. L. Farnworth, H. Leffler, U. J. Nilsson, T. Delaine, A. J. Simpson, S. J. Forbes, N. Hirani, J. Gauldie, T. Sethi, *Am. J. Respir. Crit. Care Med.* **2012**, *185*, 537.
[17] K. Takehara, Y. Koga, Y. Hachisu, M. Utsugi, Y. Sawada, Y. Saito, S. Yoshimi, M. Yatomi, Y. Shin, I. Wakamatsu, K. Umetsu, S. Kouno, J. Nakagawa, N. Sunaga, T. Maeno, T. Hisada, *Cells* **2022**, *11*, 143.
[18] A. Donato, A. Di Stefano, N. Freato, L. Bertocchi, P. Brun, *Polymers (Basel)* **2024**, *16*, 138.
[19] E. M. Dangerfield, C. H. Plunkett, A. L. Win-Mason, B. L. Stocker, M. S. M. Timmer, *J. Org. Chem.* **2010**, *75*, 5470.
[20] A. Alekseeva, R. Raman, G. Eisele, T. Clark, A. Fisher, S. Lee, X. Jiang, G. Torri, R. Sasisekharan, S. Bertini, *Carbohydr. Polym.* **2020**, *234*, 115913.
[21] S. Bertini, G. Risi, M. Guerrini, K. Carrick, A. Szajek, B. Mulloy, *Molecules* **2017**, *22*, 1214.
[22] A. Harding, C. Theisen, M. P. Deacon, S. E. Harding, *Refractive Increment Data-Book*, 1st ed., Nottingham University Press, UK **1999**.
[23] I. Christiansen-Brams, M. Meldal, K. Bock, *J. Carbohydr. Chem.* **1992**, *11*, 813.
[24] M. D'Este, D. Eglin, M. Alini, *Carbohydr. Polym.* **2014**, *108*, 239.
[25] S. A. Raw, *Tetrahedron Lett.* **2009**, *50*, 946.
[26] F. J. Wende, S. Gohil, L. I. Nord, A. Helander Kenne, C. Sandström, *Carbohydr. Polym.* **2017**, *157*, 1525.
[27] P. Farkas, S. Bystricky, *Carbohydr. Polym.* **2007**, *68*, 187.
[28] N. Veraldi, M. Guerrini, E. Urso, G. Risi, S. Bertini, D. Bensi, A. Bisio, *J. Pharm. Biomed. Anal.* **2018**, *156*, 67.
[29] L. Mauri, G. Boccardi, G. Torri, M. Karfunkle, E. Macchi, L. Muzi, D. Keire, M. Guerrini, *J. Pharm. Biomed. Anal.* **2017**, *136*, 92.
[30] S. Highsmith, J. H. Garvin, D. M. Chipman, *J. Biol. Chem.* **1975**, *250*, 7473.
[31] K. Girish, K. Kemparaju, S. Nagaraju, B. Vishwanath, *Curr. Med. Chem.* **2009**, *16*, 2261.
[32] I. Kakizaki, N. Ibori, K. Kojima, M. Yamaguchi, M. Endo, *FEBS. J.* **2010**, *277*, 1776.
[33] C. E. Schanté, G. Zuber, C. Herlin, T. F. Vandamme, *Carbohydr. Polym.* **2012**, *87*, 2211.
[34] A. García-Abuín, D. Gómez-Díaz, J. M. Navaza, L. Regueiro, I. Vidal-Tato, *Carbohydr. Polym.* **2011**, *85*, 500.
[35] P. Sindrewicz, E. A. Yates, J. E. Turnbull, L. Y. Lian, L. G. Yu, *Biochem. Biophys. Res. Commun.* **2020**, *523*, 336.
[36] P. Sindrewicz, X. Li, E. A. Yates, J. E. Turnbull, L. Y. Lian, L. G. Yu, *Sci. Rep.* **2019**, *9*, 11851.
[37] S. Fayad, R. Nehmé, M. Langmajerová, B. Ayela, C. Colas, B. Maunit, J. C. Jacquinet, A. Vibert, C. Lopin-Bon, G. Zdeněk, P. Morin, *Anal. Chim. Acta* **2017**, *951*, 140.
[38] M. C. Rodriguez, S. Yegorova, J. P. Pitteloud, A. E. Chavaroche, S. André, A. Ardá, D. Minond, J. Jiménez-Barbero, H. J. Gabius, M. Cudic, *Biochemistry* **2015**, *54*, 4462.
[39] T. J. Hsieh, H. Y. Lin, Z. Tu, B. S. Huang, S. C. Wu, C. H. Lin, *PLoS One* **2015**, *10*, e0125946.
[40] S. P. Bernhard, C. K. Goodman, E. G. Norton, D. G. Alme, C. M. Lawrence, M. J. Cloninger, *ACS Omega* **2020**, *5*, 29017.
[41] A. Lepur, E. Salomonsson, U. J. Nilsson, H. Leffler, *J. Biol. Chem.* **2012**, *287*, 21751.
[42] N. Ahmad, H. J. Gabius, H. Kaltner, S. André, I. Kuwabara, F. T. Liu, S. Oscarson, T. Norberg, C. F. Brewer, *Can. J. Chem.* **2002**, *80*, 1096.
[43] C. P. Sparrow, H. Leffler, S. H. Barondes, *J. Biol. Chem.* **1987**, *262*, 7383.
[44] H. Leffler, S. H. Barondes, *J. Biol. Chem.* **1986**, *261*, 10119.
[45] J. Hirabayashi, T. Hashidate, Y. Arata, N. Nishi, T. Nakamura, M. Hirashima, T. Urashima, T. Oka, M. Futai, W. E. G. Muller, F. Yagi, K. Kasai, *Biochim. Biophys. Acta—Gen. Subj.* **2002**, *1572*, 232.

SUPPORTING INFORMATION

Additional supporting information can be found online in the Supporting Information section at the end of this article.

How to cite this article: S. Nizzolo, E. Esposito, M.-H. Ni, L. Bertocchi, G. Bianchini, N. Freato, S. Zanzoni, M. Guerrini, S. Bertini, *Proteoglycan Res.* **2024**, *0*, e19. https://doi.org/10.1002/pgr2.19